Shaikh, Bushra; Garau Burguera, Pere; Al-Tous, Hanan; Juntti, Markku J.; Khan, Muhammad Bilal; Tirkkonen, Olav

Pilot Assignment based on AoA Information using Channel Charting in Massive MIMO Systems

Published in:
2024 IEEE 25th International Workshop on Signal Processing Advances in Wireless Communications, SPAWC 2024

DOI:
10.1109/SPAWC60668.2024.10694164

Published: 01/01/2024

Document Version
Peer-reviewed accepted author manuscript, also known as Final accepted manuscript or Post-print

Please cite the original version:
Shaikh, B., Garau Burguera, P., Al-Tous, H., Juntti, M. J., Khan, M. B., & Tirkkonen, O. (2024). Pilot Assignment based on AoA Information using Channel Charting in Massive MIMO Systems. In *2024 IEEE 25th International Workshop on Signal Processing Advances in Wireless Communications, SPAWC 2024* (pp. 166-170). (SPAWC). IEEE. https://doi.org/10.1109/SPAWC60668.2024.10694164

Pilot Assignment based on AoA Information using Channel Charting in Massive MIMO Systems

Bushra Shaikh[1,2], Pere Garau Burguera[1], Hanan Al-Tous[1], Markku Juntti[3], Bilal Muhammad Khan[2], and Olav Tirkkonen[1]

[1] Department of Information and Communications Engineering, Aalto University, Finland
[2] Department of Electronics and Power Engineering, National University of Sciences and Technology, Pakistan
[3] Centre for Wireless Communications, University of Oulu, Finland
Email: {bushra.shaikh, pere.garauburguera, hanan.al-tous, olav.tirkkonen}@aalto.fi,
markku.juntti@oulu.fi, bmkhan@pnec.nust.edu.pk

***Abstract*—We consider a multi-point channel charting (CC) based uplink pilot allocation algorithm for a multi-cell network. We create the channel chart on an offline phase and map the base station (BS) locations to charting locations. The chart provides an approximation of the geometry of the network, with imprecise but indicative distances and directions. Accordingly we model the angle of arrival (AoA) of the signal arriving at the BS from a user equipment (UE) on the CC by a probability distribution. We make use of AoA distributions on the CC to construct similarity weights between users; users nearby in the angular domain have large similarity, whereas more distant users have smaller similarity values. The points of view of all BSs are considered to create a global similarity matrix. A constrained weighted graph colouring algorithm is then applied to allocate pilots. Simulation results show that the proposed pilot allocation algorithm outperforms state of the art CC-based pilot allocation algorithms. The performance of the CC-angle based pilot allocation scheme is comparable to that obtained by using known physical locations and angle spread information.**

***Index Terms*—Multi-cell systems, pilot interference, pilot allocation, angle-of-arrival, channel charting.**

I. Introduction

Beyond 5G wireless systems depend on massive multiple-input multiple-output (mMIMO) base stations (BSs) to serve multiple user equipments (UEs) simultaneously. Accurate acquisition of channel state information (CSI) at BSs is the key to improve uplink spectral and energy efficiency. This can be achieved by proper choice of UE pilot signals. However, there are usually fewer orthogonal pilot sequences than UEs. Pilots need to be non-orthogonal and/or reused in the network, which causes pilot interference and reduces channel estimation accuracy. Many schemes have been proposed for efficient pilot reuse to minimise the impact of pilot interference [1], [2].

Many pilot assignment schemes assume knowledge of second order channel statistics such as large-scale fading coefficients, channel covariance matrices, location information, or a combination of these. Location-aware pilot allocation schemes such as in [3] build on the fact that the same pilot can be assigned to UEs with non-overlapping angle of arrivals (AoAs). This approach works well only if the angle spread of each UE is small, as is the case in line of sight (LoS) communication, which is not possible in wireless systems [4]. An improved model was considered in [5], [6], where an interval of AoAs for each UE takes into account non-line-of-sight propagation.

When true UE locations are not known, *channel charting* (CC) can be brought to play. CC exploits the spatial information existing in slowly varying channel characteristics to create a self-supervised map of UEs, which preserves UE relative position [7], and can be used for radio resource management [8], [9]. In [9], CC is used to mitigate pilot contamination in a single cell mMIMO system. In [10], the pilot allocation algorithm is extended to multi-cell mMIMO setup but the point of view of only one BS is considered. In [11], we considered CC-based pilot allocation in a multi-cell system, where user similarity is directly based on CC-distance. We concentrated on the *partial information* problem; to create a multipoint CC in the offline phase, CSI of sample UEs measured by all BSs was used, while in the online phase, only CSI measured at the serving BS was used. Pilots were allocated based on a weighted graph coloring (WGC) approach.

In this paper, in contrast to [10], [11], we concentrate on using AoA information obtained from UE and BS locations on the CC. As a CC may not preserve precise angle information between UEs, we consider an AoA-interval based interference model to capture the similarity between UEs, taking into account the points of view of all BSs and then applying WGC to allocate pilots.

II. System Model

A multi-cell mMIMO system is considered, comprising B BSs, each managing S sectors, making the total number of sectors in the system $C = SB$. Each sector is served by an M-element uniform linear array (ULA). We consider K single-antenna UEs uniformly spread across the network area. We model the channel gain of UE k in cell c on a narrowband subcarrier in terms of P multipath components (MPCs) as

$$\mathbf{h}_{c,k} = \sqrt{\beta_{b,k}} \sum_{p=1}^{P} \sqrt{A\left(\theta_{c,k}^{(p)}\right)}\, \alpha_{c,k}^{(p)}\, \mathbf{a}_M\left(\theta_{c,k}^{(p)}\right) \in \mathbb{C}^M . \quad (1)$$

Here $\beta_{b,k} = \frac{\rho_0}{d_{b,k}^{\kappa}}$ is the path loss between UE k and BS b, with $d_{b,k}$ the distance between UE k and BS b containing cell c, κ is the path loss exponent, and ρ_0 is the path loss at the reference distance of 1 m. The instantaneous small-scale fading channel gain associated with MPC p is $\alpha_{c,k}^{(p)} \in \mathbb{C}$. Path p arrives at an azimuth AoA $\theta_{c,k}^{(p)}$. The array response vector is

$$\mathbf{a}_M(\theta) = \left[1, e^{2j\pi\mu \sin\theta}, \ldots, e^{2j\pi\mu(M-1)\sin\theta}\right]^{\mathrm{T}},$$

where μ is the ULA element spacing normalized by the wavelength. The antenna gain is [12]

$$A(\theta)_{\mathrm{dB}} = G_{\max}(\theta) - \min\left\{12\left(\frac{\theta}{\theta_{3\mathrm{dB}}}\right)^2,\ A_{\max}\right\}, \quad (2)$$

where $\theta_{3\mathrm{dB}}$ is the 3 dB beamwidth, $A_{\max}$ is the maximum attenuation and $G_{\max}$ is the maximum antenna gain. The covariance matrix of UE k in cell c is $\mathbf{R}_{c,k} = \mathbb{E}\left[\mathbf{h}_{c,k}\mathbf{h}_{c,k}^{\mathrm{H}}\right]$, where the expectation is taken over small-scale fading.

We consider the one-ring channel model [2], where UEs are surrounded by rings of scatterers at close proximity. Each multi-path component arrives at the receiving antenna array after being scattered at the ring. With this model, the unnormalized covariance matrix of UE k in cell c can be found as [2]

$$r_{c,k,n,m} = \beta_{b,k} \int_{-\pi}^{\pi} A(\theta)\ e^{-j2\pi\mu(n-m)\sin(\theta)} f_{\Theta}(\theta)\, d\theta,$$

where $n, m = 0, \ldots, M-1$ denote the indices of the ULA elements, and $f_{\Theta}(\cdot)$ is the probability density function of the AoA. The AoAs for all P paths between UE k and cell c are modelled as i.i.d. uniformly distributed random variables, with distribution $\mathcal{U}\left[\theta_{c,k}^{\min},\ \theta_{c,k}^{\max}\right]$, where $\theta_{c,k}^{\min} = \bar{\theta}_{c,k} - \sqrt{3}\sigma_\theta$ and $\theta_{c,k}^{\max} = \bar{\theta}_{c,k} + \sqrt{3}\sigma_\theta$. with $\bar{\theta}_{c,k} \in [0, 2\pi]$ denoting the angle of incidence of the path arriving at cell c from UE k, and σ_θ is the angular standard deviation. The element at row n and column m of the covariance matrix of UE k at cell c can be approximated as

$$r_{c,k,n,m} \approx \frac{\beta'_{c,k}}{2\sqrt{3}\sigma_\theta} \int_{\theta_{c,k}^{\min}}^{\theta_{c,k}^{\max}} e^{-j2\pi\mu(n-m)\sin(\theta)} d\theta,$$

where $\beta'_{c,k} = \beta_{b,k} A\left(\bar{\theta}_{c,k}\right)$.

III. Channel Estimation

We consider a block-fading model. In each coherence block, the channels of active UEs are estimated at the BSs from transmitted uplink pilots. During training, K UEs transmit their pre-assigned pilot sequences of length τ, to be received in all C cells. The orthogonal sequences are $\mathbf{\Phi} = [\boldsymbol{\phi}_1, \ldots, \boldsymbol{\phi}_\tau] \in \mathbb{C}^{\tau\times\tau}$. The pilot signal transmitted by UE k is $\sqrt{\varrho}\boldsymbol{\phi}_{\pi_k}^{\mathrm{T}} \in \mathbb{C}^{1\times\tau}$, where ϱ is the power of the pilot symbols and $\pi_k \in \{1, \ldots, \tau\}$ indicates the index of the pilot assigned to UE k.

The set of UEs interfering with UE k, i.e., being assigned the same pilot, is denoted as $\mathcal{J}_k = \{j \mid j \in \mathcal{K}\backslash k,\ \pi_j = \pi_k\}$, where $\mathcal{K}$ designates the set of active UEs. Cell c receives the signal from all pilots as

$$\mathbf{Y}_c = \sum_{\rho=1}^{\tau} \mathbf{Y}_{c,\rho} + \mathbf{N},$$

where $\mathbf{N} \in \mathbb{C}^{M\times\tau}$ is additive white Gaussian noise (AWGN), and the received signal corresponding to pilot π_k is

$$\mathbf{Y}_{c,\pi_k} = \sqrt{\varrho}\left(\mathbf{h}_{c,k} + \sum_{j\in\mathcal{J}_k} \mathbf{h}_{c,j}\right)\boldsymbol{\phi}_{\pi_k}^{\mathrm{T}}. \quad (3)$$

A raw channel estimate for UE k can be found by correlating $\mathbf{Y}_c$ with $\boldsymbol{\phi}_{\pi_k}$ and normalizing the power, as [4]

$$\mathbf{y}_{c,k}^{(\mathrm{d})} = \mathbf{h}_{c,k} + \sum_{j\in\mathcal{J}_k} \mathbf{h}_{c,j} + \mathbf{n}\,. \quad (4)$$

Here $\mathbf{n}$ is normalized processed noise, with power $\frac{\sigma_n^2}{\tau\varrho}$ at each antenna, where σ_n^2 is the noise power. The first term is the desired signal, i.e., the channel gain of UE k. The second term $\sum_{j\in\mathcal{J}_k} \mathbf{h}_{c,j}$ denotes pilot interference, caused by both intra- and inter-cell UEs sharing the same pilot π_k. The covariance matrix of the processed pilot signal from UE k is

$$\mathbf{Q}_{c,k} = \mathbf{R}_{c,k} + \sum_{j\in\mathcal{J}_k} \mathbf{R}_{c,j} + \frac{\sigma_{\mathrm{n}}^2}{\tau\varrho}\mathbf{I}. \quad (5)$$

Assuming that $\mathbf{R}_{c,k}$ is known and that $\mathbf{Q}_{c,k}$ can be estimated, cell c applies linear minimum mean square error (LMMSE) estimation to find the channel estimate of UE k as

$$\hat{\mathbf{h}}_{c,k} = \mathbf{R}_{c,k}\, \mathbf{Q}_{c,k}^{-1}\mathbf{y}_{c,k}^{(\mathrm{d})}. \quad (6)$$

The channel estimation error is denoted as $\tilde{\mathbf{h}}_{c,k} = \mathbf{h}_{c,k} - \hat{\mathbf{h}}_{c,k}$, where $\tilde{\mathbf{h}}_{c,k} \sim \mathcal{CN}(0, \tilde{\mathbf{R}}_{c,k})$, and its covariance matrix is [2]

$$\tilde{\mathbf{R}}_{c,k} = \mathbf{R}_{c,k} - \mathbf{R}_{c,k}\mathbf{Q}_{c,k}^{-1}\mathbf{R}_{c,k}. \quad (7)$$

The normalized mean square error (NMSE)

$$\mathbf{NMSE} = \frac{1}{K}\sum_{c=1}^{C}\sum_{k\in\mathcal{I}_c} \frac{\mathrm{Tr}\left(\tilde{\mathbf{R}}_{c,k}\right)}{\mathrm{Tr}\left(\mathbf{R}_{c,k}\right)}. \quad (8)$$

is used to assess the quality of the channel estimation of all UEs with respect to their serving cells.

IV. Channel Charting

CC [7] is an unsupervised machine learning scheme attempting to convey high-dimensional radio properties onto a low-dimensional embedding, while preserving the local geometry of the UEs. Here we consider CCs constructed from CSI features obtained from channel covariance matrices, as they capture large-scale spatial geometry. A distance between covariance matrices $\mathbf{R}_i$ and $\mathbf{R}_j$ can be used as a proxy for the true distance between UEs j and k. E.g., the correlation matrix distance (CMD) or the log-Euclidean distance may be used:

$$d_{\mathrm{CMD}}(\mathbf{R}_i, \mathbf{R}_j) = 1 - \frac{\mathrm{Tr}\left(\mathbf{R}_i\mathbf{R}_j\right)}{\|\mathbf{R}_i\|_{\mathrm{F}}\|\mathbf{R}_j\|_{\mathrm{F}}}, \quad (9)$$

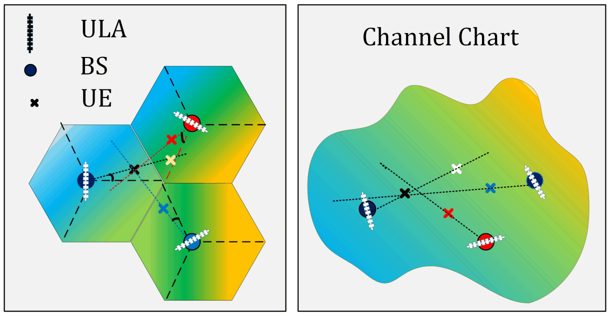

Fig. 1: (Left): A Multi-cell system. (Right) CC of the systems, BSs are located on the CC.

$$d_{\text{LogEuc}}(\mathbf{R}_i, \mathbf{R}_j) = \|\log(\mathbf{R}_i) - \log(\mathbf{R}_j)\|_{\text{F}}\,. \tag{10}$$

Multi-point CC (MPCC) [13] extends the idea of independent single-point CCs at each cell into a framework in which multiple mMIMO cells collectively learn a chart based on partial CSI, i.e., the CSI related to each UE is not known by all cells. The centralized unit obtains a global matrix $\mathbf{D}$ by merging local dissimilarity matrices $\mathbf{D}_c$ of the cells,

$$\mathbf{D} = \sum_{c}^{C} \tilde{\mathbf{F}}_c \odot \mathbf{D_c}, \tag{11}$$

where $\mathbf{D}_c$ is obtained by arranging the pairwise values at cell c from (9) or (10) into a matrix, with normalized weighting factor

$$\tilde{f}_{c,i,j} = \frac{f_{c,i,j}}{\sum_{c'} f_{c',i,j}}, \text{ and } f_{c,i,j} = \left(\min\{\beta'_{c,i},\, \beta'_{c,j}\}\right)^2.$$

After constructing the global dissimilarity matrix, the CC is found with a dimensionality reduction technique such as t-distributed stochastic neighbor embedding (t-SNE). The quality of the CC is assessed by measuring its capacity of preserving the geometry of the true UE locations. Kruskal's stress (KS) measures the distance distortion between UE locations and chart locations, where trustworthiness (TW) and continuity (CT) measure the quality of neighborhood preservation between points.

Placing out-of-sample (OoS) UEs onto the CC can be done by exploiting the offline MPCC. When a UE joins the network, its chart location can be estimated by averaging the CC locations of its $\mathscr{K}$ nearest neighbours (KNN) in feature space.

The CC location of cell c is determined by averaging out the CC locations of the $\mathscr{I}$ UEs in the cell with largest $\beta^{'}_{c,k}$. The antenna orientation at cell c is assumed to be orthogonal to the line joining the cell location and the UE with largest $\beta^{'}_{c,k}$ in the cell. A multi-cell multi-sector setup is depicted in Figure 1. In the physical domain, two UEs have the same AoA with respect to one ULA in a BS and the other pair of UEs are at LoS with another ULA in other BS. This AoA relation need to be analyzed in the CC domain. We define the distance in phase difference between two UEs with respect to the same cell based on physical locations as

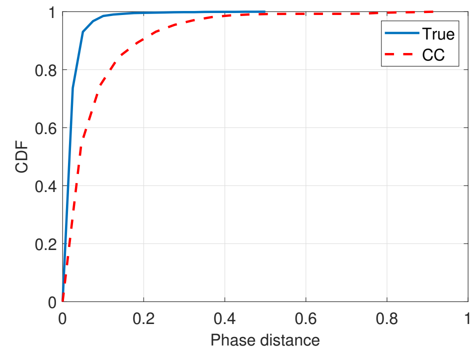

Fig. 2: The CDF of the pairwise phase distance on the physical and CC domains of the 5 nearest neighbours based on physical location.

$$\delta_{c,i,j} = |\sin(\theta_{c,i}) - \sin(\theta_{c,j})|\,,$$

where $\theta_{c,i}$ is the azimuth AoA of UE i at cell c and the corresponding absolute phase difference in the CC as

$$\eta_{c,i,j} = |\sin(\psi_{c,i}) - \sin(\psi_{c,j})|\,,$$

with $\psi_{c,i}$ is the azimuth AoA of UE i at cell c based on their CC locations. We consider the KNN based on the physical location for each point in a data set and investigate the distributions of the CC-phase and true phase distances. Figure 2 shows the CDF of the angle distribution considering five nearest neighbours. The angle distance on the CC has a larger spread, indicating that the CC does not precisely preserve phase differences.

V. Pilot Allocation

We consider pilot allocation based on a WGC approach, aiming to minimize the total interference in the network by a τ-WGC algorithm, such that one colour (i.e., pilot) is assigned for each vertex (i.e., UE). Mathematically, an undirected weighted graph is defined by $G = (\mathcal{V}, \mathcal{E})$ where the vertex set $\mathcal{V}$ represents the UEs and the edge set $\mathcal{E}$ represents the interference weight between two UEs. First, a similarity matrix $\mathbf{W}_c$ for each cell in the network is created, and then the network point of view is obtained by taking the mean of all views. The network weight matrix is obtained as $\mathbf{W} = \frac{1}{2}\sum_c \left(\mathbf{W}_c + \mathbf{W}_c^{\text{T}}\right)$, where the second term is used to obtain a symmetric matrix.

The degree of vertex i is defined as $\varrho_i = \sum_{j=1}^{K} w_{i,j}$. When greedy colouring is considered, the vertices are sorted w.r.t their degrees and first τ unique pilots are assigned to the τ UEs with highest degrees. The remaining UEs are considered in decreasing order of ϱ one-by-one. The cost of pilot k is found by adding the weights of all vertices assigned the pilot ϕ_k; the pilot with the least cost is assigned to the next unassigned UE.

A. Channel Charting Based AoA Similarity

UEs with mutually non-overlapping AoAs can be assigned the same pilots [4]. However, each cell has its own opinion on the AoA relation between two UEs as illustrated in Figure 1. Hence the opinions of all BSs need to be considered when measuring the interference weight between two UEs.

Assuming the physical locations are not available, the similarity between two UEs at cell c based on their CC AoAs can be computed as [3]

$$w_{c,i,j} = \begin{cases} 0 & \text{if } i = j, \\ \left|\frac{\sin(\pi r M \Omega_{c,i,j})}{M \sin(\pi r \Omega_{c,i,j})}\right|^2 & \text{if } i,\ j \in \mathcal{I}_c, \\ \left(\frac{\beta'_{c,j}}{\beta'_{c,i}}\right)^{\alpha} \left|\frac{\sin(\pi r M \Omega_{c,i,j})}{M \sin(\pi r \Omega_{c,i,j})}\right|^2 & \text{if } i \in \mathcal{I}_c,\ j \notin \mathcal{I}_c, \\ 0 & \text{if } i,\ j \notin \mathcal{I}_c, \end{cases} \tag{12}$$

where $\Omega_{c,i,j} = \sin\psi_{c,i} - \sin\psi_{c,j}$. In creating the similarity of a cell, it is important to differentiate between a UE served in the cell and another UE that is not served by the cell [6].

Since CC does not preserve angle between UEs, we model the signal arriving at the antenna of cell c from UE i using the CC locations as $\psi_{c,i} \sim \mathcal{U}\left[\psi_{c,i}^{\min},\ \psi_{c,i}^{\max}\right]$, with $\psi_{c,i}^{\min} = \bar{\psi}_{c,i} - \sqrt{3}\sigma_\psi$, $\psi_{c,i}^{\max} = \bar{\psi}_{c,i} + \sqrt{3}\sigma_\psi$, $\bar{\psi}_{c,i}$ is the AoA at cell c from the CC location of UE i, and σ_ψ models both the spread of the AoA and error due to CC. We compute the angle similarity based on AoA using CC with uncertainty model as [6]

$$\nu_{c,i,j} = \frac{\left|\left[\psi_{c,i}^{\min},\ \psi_{c,i}^{\max}\right] \cap \left[\psi_{c,j}^{\min},\ \psi_{c,j}^{\max}\right]\right|}{2\sqrt{3}\sigma_\psi}.$$

We define the similarity of UEs i and j at cell c based on CC AoAs as

$$w_{c,i,j} = \begin{cases} 0 & \text{if } i = j, \\ \nu_{c,i,j} & \text{if } i,\ j \in \mathcal{I}_c, \\ \left(\frac{\beta'_{c,j}}{\beta'_{c,i}}\right)^{\alpha} \nu_{c,i,j} & \text{if } i \in \mathcal{I}_c,\ j \notin \mathcal{I}_c, \\ 0 & \text{if } i,\ j \notin \mathcal{I}_c, \end{cases} \tag{13}$$

where α and σ_ψ are tuning parameters.

B. Benchmark Methods: CC Based

A simple greedy algorithm is proposed in [10] to allocate the pilots for MPCC. This strategy is realized by first selecting a random UE, which is allocated first orthogonal pilot $\boldsymbol{\phi}_1$. Next, its closest neighbor in terms of CC distance is allocated the next available pilot $\boldsymbol{\phi}_2$. The process continues till all τ orthogonal pilots are allocated and repeated for the remaining UEs. This increases the CC distance between the UEs with the same pilots and thereby reduces the pilot interference.

C. Benchmark Methods: Physical Location Based Allocation

The pilot allocation algorithms most related to our work are based on creating the similarity using physical locations and then apply a WGC scheme. The cell similarity based on the physical location can be created as follows:

- AoA based [3]: The similarity between two UEs at cell c based on their AoAs and and path loss is computed using (12), by replacing the CC AoAs with true AoAs.
- AoA interval based: The similarity between two UEs at cell c based on their AoAs, path loss, and angle spread is computed using (13), by replacing the CC AoAs with true AoAs.

TABLE I: Simulation parameters.

Parameter	Value
Num. of ant. M	32
Inter-site distance	500 m
Carrier frequency f_c	2 GHz
Bandwidth	50 MHz
BS height	25 m
Norm. ant. spa. μ	0.5
$\beta_{b,k}$ [dB]	$13.54 + 39.08 \log_{10} d_{b,k} + 20 \log_{10} f_\mathrm{c}$
Ang. dev. σ_θ	$10°$
Num. of UEs	4000 (offline), 1000 (online)
UE height	1.5 m
$G_{\max}$, $A_{\max}$	0 dB, 30 dB
Num. of pilots τ	$[10,\ 80]$
Noise power σ_n^2	-90 dBm
Signal power	23 dBm

VI. Simulation results

We consider a mMIMO system consisting of $B = 7$ BSs, each with $S = 3$ sectors in an urban macro (UMa) 3GPP propagation model [14]. The simulation parameters are summarized in Table I. The channel covariance matrices of all UEs are generated to compute the dissimilarity of all cells/BSs, which are then merged using (11). We consider the following principles:

- Sector selection CC (SSCC): The dissimilarity of each sector-level covariance matrix is created using CMD and are merged using sector selection method [10].
- Multi-sector CC (MSCC): The multi-sector-level covariance matrix is used to estimate the dissimilarity matrix for each BS assuming phase coherence between sectors using the Log-Euclidean distance. These are merged to get a global dissimilarity matrix.

With the merged dissimilarity matrix, we apply t-SNE to obtain the MPCC. Figure 3 shows the CCs and corresponding physical locations. The MSCC has better quality in terms of TW, CT and KS compared to SSCC. The Log-Euclidean shows better quality compared to CMD [8].

The MSCC is used to create the similarity based on AoA (12) and AoA interval overlap (13) and the WGC greedy algorithm is applied to allocate the pilots. The parameters α and σ_ψ are tuned to get the best performance. To benchmark the performance of the proposed CC based pilot allocations, we consider the following approaches:

- Random: The pilots are allocated randomly [1].
- AoA based: The similarity is computed as in (12) by replacing the CC AoAs by true AoAs and then the WGC greedy algorithm is applied.
- AoA interval overlap based: The similarity is computed as in (13) by replacing the CC AoAs and the uncertainty σ_ψ by true AoAs and σ_θ, and then the WGC is applied.
- The SSCC and MSCC are used and the pilots are allocated using the greedy approach in [10].

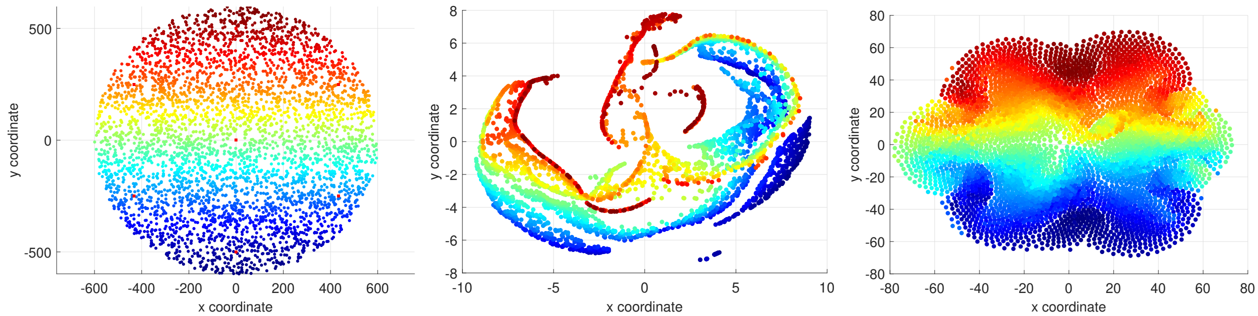

Fig. 3: (i) Physical Locations of UEs. (ii) SSCC as in [10]. (iii) MSCC. CC locations are marked by colours corresponding to the physical locations in (i).

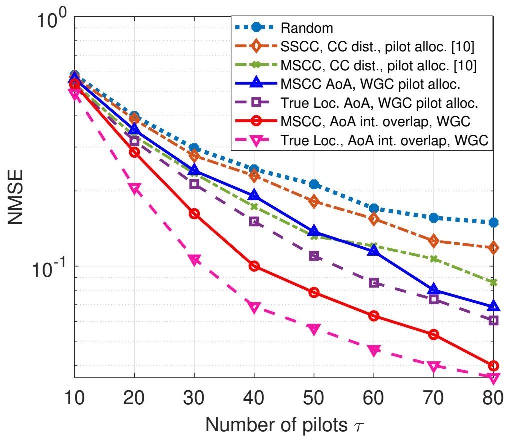

Fig. 4: NMSE performance of different pilot allocation schemes as a function of the number of pilots, considering 1000 UEs.

Figure 4 shows the NMSE (8) as a function of pilot length τ for the proposed CC based approach compared to the benchmark schemes. The legend `"SSCC, CC dist., pilot alloc. in [10]"` implies that the pilots are allocated as in [10] using CC distance of SSCC and `"MSCC, AoA, pilot alloc. WGC"`, means that AoA of MSCC is used to create similarity and the pilots are allocated using WGC. The performance of the MSCC interval overlap outperforms other CC based schemes, and is comparable to those using physical locations based interval overlap. Applying the algorithm in [10] on enhanced CC, i.e., MSCC, improves the NMSE performance as expected. Considering the points of view of all cells clearly improves the NMSE performance.

VII. Conclusions

In this paper, we consider a pilot allocation scheme based on weighted graph coloring using channel charting (CC) in a multi-cell massive MIMO system. The base stations (BSs) locations are mapped to the CC using a simple $\mathscr{I}$ nearest neighbor approach considering the path-loss of the served users in the cell. The multi-point CC provides a global network view of the geometry. However, the CC may not preserve the precise AoA information between UEs. In this regard, we have utilized a probabilistic model for AoA distribution on the CC. The performance of the CC based pilot allocation is comparable to the one based on physical location and angle spread information.

Acknowledgements

This work was funded by the Research Council of Finland (RCF) grant 345109, by CHIST-ERA project CHASER (CHIST-ERA-22-WAI-01) through RCF grant 359837, the RCF via 6G Flagship grant 318927, and the Higher Education Commission of Pakistan.

References

[1] T. L. Marzetta, "Noncooperative cellular wireless with unlimited numbers of base station antennas," *IEEE Trans. Wireless Commun.*, vol. 9, no. 11, pp. 3590–3600, 2010.
[2] E. Björnson, J. Hoydis, and L. Sanguinetti, *Massive MIMO Networks: Spectral, Energy, and Hardware Efficiency*. Hanover, MA, USA: Now Publishers Inc., 2018.
[3] N. Akbar, S. Yan, N. Yang, and J. Yuan, "Location-aware pilot allocation in multicell multiuser massive MIMO networks," *IEEE Trans. Veh. Technol.*, vol. 67, no. 8, pp. 7774–7778, 2018.
[4] H. Yin, D. Gesbert, M. Filippou, and Y. Liu, "A coordinated approach to channel estimation in large-scale multiple-antenna systems," *IEEE J. Sel. Areas Commun.*, vol. 31, no. 2, pp. 264–273, 2013.
[5] L. S. Muppirisetty, T. Charalambous, J. Karout, G. Fodor, and H. Wymeersch, "Location-aided pilot contamination avoidance for massive MIMO systems," *IEEE Trans. Wireless Commun.*, vol. 17, no. 4, pp. 2662–2674, 2018.
[6] P. Li, Y. Gao, Z. Li, and D. Yang, "User grouping and pilot allocation for spatially correlated massive MIMO systems," *IEEE Access*, vol. 6, pp. 47 959–47 968, 2018.
[7] C. Studer, S. Medjkouh, E. Gonultaş, T. Goldstein, and O. Tirkkonen, "Channel Charting: Locating users within the radio environment using channel state information," *IEEE Access*, vol. 6, pp. 47 682–47 698, 2018.
[8] P. Kazemi, H. Al-Tous, T. Ponnada, C. Studer, and O. Tirkkonen, "Beam SNR prediction using channel charting," *IEEE Trans. Veh. Technol.*, vol. 72, no. 10, pp. 13 130–13 145, 2023.
[9] L. Ribeiro, M. Leinonen, H. Al-Tous, O. Tirkkonen, and M. Juntti, "Channel charting aided pilot reuse for massive MIMO systems with spatially correlated channels," *IEEE Open J. Commun. Soc.*, vol. 3, pp. 2390–2406, 2022.
[10] L. Ribeiro, M. Leinonen, I. Rathnayaka, H. Al-Tous, and M. Juntti, "Channel charting aided pilot allocation in multi-cell massive MIMO mMTC networks," in *Proc. IEEE SPAWC*, 2022, pp. 1–5.
[11] B. Shaikh, P. Garau Burguera, H. Al-Tous, M. Juntti, B. M. Khan, and O. Tirkkonen, "Channel charting based pilot allocation in MIMO systems," in *IEEE PIMRC*, Sept 2024, pp. 1–7.
[12] D. G. Riviello, F. D. Stasio, and R. Tuninato, "Performance analysis of multi-user MIMO schemes under realistic 3GPP 3-D channel model for 5G mmWave cellular networks," *Electronics*, vol. 11, no. 3, 2022.
[13] J. Deng, S. Medjkouh, N. Malm, O. Tirkkonen, and C. Studer, "Multipoint channel charting for wireless networks," in *Proc. Asilomar Conf. Sign., Syst., Comput.*, Oct. 2018, pp. 286–290.
[14] 3GPP, "Study on channel model for frequencies from 0.5 to 100 GHz," TS 38.901, Jan. 2018, version 14.3.0.